Available online at www.sciencedirect.com
SCIENCE DIRECT®
Journal of Chromatography A, 1064 (2005) 107–114
JOURNAL OF CHROMATOGRAPHY A
www.elsevier.com/locate/chroma

Automated analysis of individual particles using a commercial capillary electrophoresis system

Hossein Ahmadzadeh, Rajat Dua, Andrew D. Presley, Edgar A. Arriaga*

Department of Chemistry, University of Minnesota, 207 Pleasant Street S.E., Minneapolis, MN 55455, USA

Received 13 July 2004; received in revised form 18 November 2004; accepted 6 December 2004
Available online 25 December 2004

Abstract

Capillary electrophoretic analysis of individual submicrometer size particles has been previously done using custom-built instruments. Despite that these instruments provide an excellent signal-to-noise ratio for individual particle detection, they are not capable of performing automated analyses of particles. Here we report the use of a commercial Beckman P/ACE MDQ capillary electrophoresis (CE) instrument with on-column laser-induced fluorescence (LIF) detection for the automated analysis of individual particles. The CE instrument was modified with an external I/O board that allowed for faster data acquisition rates (e.g. 100 Hz) than those available with the standard instrument settings (e.g. 4 Hz). A series of eight hydrodynamic injections expected to contain 32 ± 6 particles, each followed by an electrophoretic separation at $-300\,\mathrm{V\,cm^{-1}}$ with data acquired at 100 Hz, showed 28 ± 5 peaks corresponding to 31.9 particles as predicted by the statistical overlap theory. In contrast, a similar series of hydrodynamic injections followed by data acquisition at 4 Hz revealed only 8 ± 3 peaks suggesting that the modified system is needed for individual particle analysis. Comparison of electropherograms obtained at both data acquisition rates also indicate: (i) similar migration time ranges; (ii) lower variation in the fluorescence intensity of individual peaks for 100 Hz; and (iii) a better signal-to-noise ratio for 4 Hz raw data. S/N improved for 100 Hz when data were smoothed with a binomial filter but did not reach the S/N values previously reported for post-column LIF detection. The proof-of-principle of automated analysis of individual particles using a commercially available CE system described here opens exciting possibilities for those interested in the study and analyses of organelles, liposomes, and nanoparticles.

Keywords: Individual particle analysis; Capillary electrophoresis; Fluorescence detection; Latex microspheres

1. Introduction

Colloidal particles ranging in size from several nanometers to several micrometers such as biological vesicles are important in medicine, biology, biotechnology and the environment. The surfaces of these particles either have electric charge or become charged when they are in electrolyte solutions. Therefore, electrophoretic methods have been used for the separation and analysis of this class of particles. Among different techniques, capillary electrophoresis (CE) appears to be well suited for the electrophoretic analysis of particles [1]. CE has been used for the analysis of gold colloidal particles [2], polymer particles [3], liposomes [4], mitochondria [5], viruses and bacteria [6,7].

One of the attractive features of commercial CE instruments is that they are capable of performing sequential analysis of the same sample and automated analysis of multiple samples. New specialized CE instruments with arrays of capillaries further increase sample analysis versatility and throughput [8,9]. It is desirable to use these automation features in the analysis of colloidal particles. There are reports describing the use of commercial instruments for the analysis of particles and liposomes [1,10]. In these reports the analyzed colloidal particles migrated as zones several seconds wide. For these zones, band broadening usually results from the electrophoretic dispersion of particles caused by either heterogeneity in size or surface composition that leads

* Corresponding author. Tel.: +1 612 624 8024; fax: +1 612 626 7541.
E-mail address: arriaga@chem.umn.edu (E.A. Arriaga).

0021-9673/$ – see front matter © 2004 Elsevier B.V. All rights reserved.
doi:10.1016/j.chroma.2004.12.018

to heterogeneity in electrophoretic mobility [3,11,12]. Other contributions to band broadening such as diffusion of the particles, injection plug length, detector path length, and adsorption of the particles onto the capillary wall can be usually neglected. In these separations, the fact that the average electrophoretic mobility and not individual particle mobilities is determined may be limiting because, unless the particles are truly homogeneous, there may be several combinations of particles in the sample that will lead to the same detector response. Heterogeneity in particle electrophoretic mobility would be better characterized if individual particles were analyzed. In addition, particle analyses carried out in commercial CE systems require a high number density of particles which may result in particle–particle interactions complicating the analysis [12]. Therefore, to characterize the heterogeneity expected in particle samples and to reduce the possibility of particle–particle interactions, CE analyses should be performed with diluted suspensions of particles that allow for individual particle analysis.

We have previously reported the analysis of individual latex particles using a custom-built CE instrument with a post-column laser-induced fluorescence (LIF) detector [3]. In this instrument the data acquisition rate and the detector response time were fast enough to detect individual particles that took <100 ms to travel through the post-column LIF detector comprised of a laser beam focused at the exit of the separation capillary housed within a sheath flow cuvette [13]. Similarly, commercial CE systems with on-column detectors comprised of a laser beam focused through the separation capillary, would be adequate for individual particle detection if they were configured for fast data acquisition rates, had adequate detector response time, and had processing software for analysis of peaks corresponding to individual particles. Unfortunately, most commercial instruments are configured for the analysis of relatively wide peaks and may not be suitable for detecting the narrow peaks associated with individual particle analysis. Commercial instruments with faster data acquisition rates would be highly desirable for such analyses and this would make it possible to carry out automated CE analyses of individual particles.

In this paper, we are reporting, for the first time, the use of a commercial CE system for automated analysis of individual particles. Directly interfacing the output of the photomultiplier tube of the commercial CE system with an external fast data acquisition board allowed us to reliably detect individual particles and automatically perform multiple analyses of sequential injections of samples of latex particles in suspension.

2. Reagents and methods

2.1. Reagents

Sucrose and ethanol were purchased from Fisher Scientific (Pittsburgh, PA, USA). HEPES, *N*-[2-hydroxyethyl]-piperazine-*N*-[ethanesulfonic acid], was purchased from Sigma (St. Louis, MO, USA) and KOH was from Aldrich (Milwaukee, WI, USA). Fluorescein was purchased from Molecular Probes (Eugene, OR, USA). CE separation buffer contained 10 mM HEPES and 250 mM sucrose, adjusted to pH 7.4 with KOH. All buffers were made with Milli-Q deionized water and filtered using 0.22 μm filter before being used. A stock solution of 1 mM fluorescein was made in ethanol and diluted with running buffer immediately prior to use.

Fluorescently-labeled latex particles were purchased from Polysciences Inc. (Warrington, PA, USA). The number of particles per milliliter (N) was calculated using the following equation:

$$N = \frac{6W \times 10^{12}}{\pi\rho\phi^3} \quad (1)$$

where W is the solid weight of particles per unit volume of suspension ($g\,mL^{-1}$), ϕ is the particle diameter (μm), and ρ is the particle density ($g\,mL^{-1}$). For 1 μm diameter particles with $\rho = 1.05\,g\,mL^{-1}$, $W = 0.025\,g\,mL^{-1}$, N is calculated to be 4.5×10^{10} particles mL^{-1}. For CE analysis, particles were diluted to 4.5×10^6 particles mL^{-1} with a solution containing 500 mM sucrose, 10 mM HEPES, density = $1.06 \pm 0.01\,g\,mL^{-1}$. The final density of the particle suspension after sucrose addition closely matches the density of the latex particles. This prevents settling of the latex particles in the suspension and allows for multiple sampling from the same suspension for a longer period of time.

2.2. Capillary electrophoresis

The CE-LIF system used in these studies was a Beckman Coulter P/ACE MDQ system (Fullerton, CA, USA). For excitation, the LIF detector uses a 488 nm line of a 3 mW argon-ion laser that is directed to a detector window using a fiber optic. Fluorescence is collected using a ball lens and then filtered with a laser filter and a 520DF20 interference filter (520 ± 10 nm), and sent to a photo multiplier tube (PMT). The analog PMT output was: (i) processed by the commercial instrument at 4 Hz; or (ii) sent to a data acquisition board in a different computer that allowed for data acquisition at 100 Hz.

For option (i), the MDQ was operated in the "High Resolution" mode. This mode is recommended for a more accurate description of electropherograms containing narrow features [14]. For option (ii), it was necessary to redirect the PMT output with a BNC cable to an external I/O board (PCI-MIO-16XE-50, National Instruments, Austin, TX, USA) installed in a G3 Macintosh computer. Fig. 1 is a diagram of option (ii) illustrating the interface of the CE system with the external I/O board. The I/O board was controlled using an in-house written Labview program (National Instruments), *filegenr.vi*, that also saves the data into the G3 Macintosh hard drive (electronic file available upon request). The procedure to collect data at 100 Hz, consisted of starting the Labview program

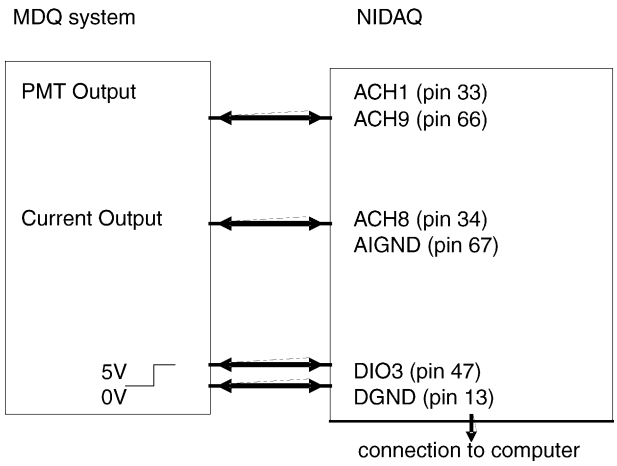

Fig. 1. Schematic representation of the interface between the Beckman P/ACE MDQ CE system and a NIDAQ (National Instrument Data Acquisition Board). The experiment was controlled with LabView version 5.0. The NIDAQ was used in a differential configuration mode. For example, pin 34 was connected to signal and pin 67 was connected to virtual ground.

(*filegenr.vi*) in the Macintosh computer followed by the initiation of the "*CE-run method*" written in Karat 32, which is the proprietary software used by the MDQ instrument (electronic file available upon request). At the beginning of a run, a "relay on/off" command in the "CE-run method" caused the relay terminal on the commercial CE instrument (Fig. 1) to change state from 0 to 5 V. The relay at the "high" state was sensed by the digital input (DI03/DIGND) in the external I/O board. A "high" state at this digital input then triggered the sequence: (i) start a new file; (ii) write data into a new file that is continually saved into the Macintosh hard drive.

Separations were performed using a 50 μm i.d., 365 μm o.d. poly(acryloylaminopropanol) coated capillary [15,16] which has been previously used in the CE-LIF analysis of particles [3]. The total capillary length and the length to the detection window were 31 and 21 cm, respectively. Using the current monitoring method [15,17], the EOF of the coated capillary at the beginning of the experiments was $(1.1 \pm 0.1) \times 10^{-5}$ cm^2 V^{-1} s^{-1}. Pressure injections (10 psi for 5 s) introduced 7 nL of the particle suspension into the capillary. Roughly, this corresponds to 32 ± 6 particles per injection. The capillary was reconditioned between consecutive runs by pressure-driven flushing (20 psi) for 2 min each of water, methanol, water and CE buffer. Separation was performed at -300 V cm^{-1} and data acquisition was carried out at either 4 or 100 Hz as described above.

2.3. Data analysis

Igor Pro software (Wavemetrics, Lake Oswego, OR, USA) was used for data analysis. Tabulation of peak intensities and migration times for individual peaks was performed using an in-house-written Igor procedure, PickPeaks2, which is similar to a previously reported procedure [4] with slight modifications that improves processing speed (available upon request). The program was set to select those peaks larger than a threshold equal to five times the standard deviation (S.D.) of the background. The electrophoretic mobility (μ) corresponding to each peak was calculated using the formula $\mu = L_d/Et_m$, where L_d is the length to the detector, E is the electric field calculated from the applied voltage (V) and the total capillary length (L_t), ($E = V/L_t$), and t_m is the migration time.

3. Results and discussion

Automated CE analysis of latex particles was carried out using a commercial instrument collecting data either at 4 or 100 Hz. For the latter, the PMT output was directed to an external I/O board. In both instances, a sequence of eight CE runs proceeded continually, with data being collected in separate files for each run without additional user input, and without additional sample handling between runs. In a previous report [3], we needed to homogenize the microsphere suspension before each CE injection in order to prevent settling and bias in the number of detected particles. In this report, we suspended particles in an isodense sucrose solution in order to prevent settling and take full advantage of the automation provided by the commercial instrument. Fig. 2A shows examples of electropherograms recorded at 4 and 100 Hz resulting from the analysis of 1.0 μm diameter fluorescently-labeled latex particles. As previously reported for the analysis of individual particles, particles are detected in a well-defined migration time window [3]. Previous evidence suggests that particle-to-particle variation in migration time is mainly an indication of electrophoretic mobility heterogeneity within the sampled particles [3]. Fig. 2B is a 30 s expansion from Fig. 2A. This expansion further illustrates that the number of detected particles and the individual peak widths are different when data are acquired at 4 and 100 Hz. Using the higher data acquisition rates more particles are detected and peak widths are narrower. These topics are discussed below.

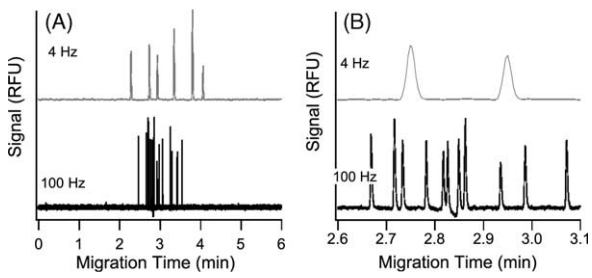

Fig. 2. Representative electropherograms of 1 μm latex particles. Panel A: the entire migration time window for data collected at 4 Hz (trace 4 Hz), and 100 Hz (trace 100 Hz). Panel B: the expansion of a region shown in part A for 4 Hz (trace 4 Hz), and 100 Hz (trace 100 Hz). Particles were suspended in 500 mM sucrose and 10 mM HEPES. CE buffer was 10 mM HEPES, 250 mM sucrose pH 7.4. Capillary length was 31 cm (21 cm to the detector) and the applied voltage was -300 V cm^{-1}. The capillary was AAP coated. Suspension injection was performed at 10 psi for 5 s.

Table 1
Number of peaks and individual signal intensity variation

	Run number								Average ± S.D.
	1	2	3	4	5	6	7	8	
Number of peaks (100 Hz)	16	28	33	27	30	28	32	27	28 ± 5
Number of peaks (4 Hz)	6	4	8	11	10	5	11	7	8 ± 3
Intensity-R.S.D. (100 Hz)	33	25	20	24	22	24	20	26	
Intensity-R.S.D. (4 Hz)	40	55	65	35	40	70	65	40	

The relative standard deviations of the individual peak intensities (intensity-R.S.D.) at these sampling frequencies are also reported.

3.1. Number of detected particles

As suggested in Fig. 2B, less peaks are detected at 4 Hz than at 100 Hz. Table 1 tabulates the results of eight consecutive injections from the same particle suspension at each data acquisition rate. On average, 28 and 8 peaks were detected when using 100 and 4 Hz data acquisition rates, respectively. A *t*-test comparison shows that the two sampling rates provide results that are statistically different with a 99% confidence level [18]. As described in the Experimental Section, from the particle number density and the injected volume, each electropherogram is expected to consist of 32 ± 6 particles. This error was estimated by propagation of errors; the relative errors for particle content (4%), sample dilutions (2%), hydrodynamic pressure (5%) and uncertainties in the constants (e.g. a change by 1 μm in a 50 μm i.d. capillary corresponds to 8% error in the injection volume) were included in this calculation. A direct peak count would suggest that 88 ± 12% of the expected number of particles were detected at 100 Hz (28 ± 5 detected particles out of 32 ± 6 injected particles). Similarly at 4 Hz, direct peak count would suggest that only 25 ± 10% of the total number of particles are detected (8 ± 3 detected particles out of 32 ± 6 injected particle) (see Table 1).

The lower number of detected versus predicted particles may be indicative of multiple component peaks. For data acquired at 4 Hz using the software package included in the commercial instrument, the presence of multiple component peaks is expected, since this software has been optimized for the analysis of conventional electropherograms where typical peak widths are in the order of seconds. In particular, this software uses data bunching (i.e. data points are averaged to represent one point in the processed electropherogram) [14] that will make impossible to detect separate particles if they migrate out within 250 ms of each other. For data acquired at 100 Hz, the appearance of multiple component peaks is mainly statistical and will be discussed in Section 3.3.

3.2. Peak width

The peak width histogram of the data pooled from eight consecutive runs for each data acquisition rate is shown in Fig. 3. The pooled data for 100 Hz have a FWHM of 208 ± 78 ms (average ± S.D.) with a median of 215 ms. The peak width of a single particle is associated with the traveling time of the particle through the laser beam of the on-column detector. This width (e.g. ∼208 ms) is not affected by other common broadening phenomena (e.g. diffusion, sample plug length, and interactions with the capillary walls) observed in chromatographic or electrophoretic separations [3]. Instead, they may have an effect on the observed migration time of a given particle. Thus, the spread of the migration time of the detected individual particles (cf. Fig. 2) is analogous to the peak widths observed for a collection of particles in electropherograms that do not have sufficient resolution. The causes of peak broadening in these electropherograms have been discussed elsewhere and will not be addressed here [3,19].

The widest peaks in the data collected at 100 Hz are not the result of multiple component peaks because the Igor algorithm used to calculate this parameter splits these peaks into narrower peaks (e.g. shoulder peak marked with (*) in Fig. 3B). These narrow peaks have typically a FWHM <150 ms and appear at the low end of the peak width distribution (Fig. 3A, 100 Hz). Narrow peaks have been included in particle counting but excluded in the calculation of the peak width average, standard deviation, and median described above.

The peak width distribution from data collected at 4 Hz is clearly different and non-overlapping with the distribution observed for data collected at 100 Hz (Fig. 3, panel A). The FWHM of this distribution is 810 ± 540 ms (average ± S.D.) with a median of 710 ms. Since the same detector configuration is used for both data acquisition rates, the differences between distributions are attributed to dif-

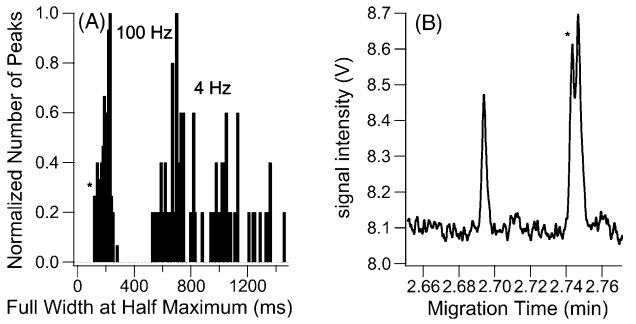

Fig. 3. Peak widths distribution. Panel A is the FWHM for peaks detected at 100 and 4 Hz. Data were pooled from eight successive runs for each data acquisition rate. All the experimental conditions are the same as in Fig. 2. Panel B is a multiple peak with a narrow shoulder. The shoulder in panel B (*) is also shown in panel A.

ferences in data processing. At 100 Hz, the PMT output is digitized and then analyzed using the Igor Pro routines described in Section 2.3. The digitization process is not expected to introduce any additional peak broadening because this data acquisition board has a rise time of 2 V μs^{-1}, which is at least three orders of magnitude faster than the observed peak widths. On the other hand, data processing at 4 Hz is done with proprietary software of the instrument manufacturer. The "high resolution mode" was used in these measurements because it provides 'faster' response, which would favor detection of individual particles. Even when using the "high resolution mode", a combination of data bunching, digital filtering, and possibly additional electronic filtering (i.e. longer detector response time resulting from additional electronic processing from the PMT output) seem to be causing additional broadening. Unfortunately, it is not feasible to tease apart the relevance of these broadening sources because the actual software algorithm and electrical signal are proprietary.

Assuming that data bunching has been optimized to capture all the information from the analog detector output (i.e. zero misses), individual particles will be detected if they are migrating out at least 250 ms apart (i.e. 4 Hz data acquisition rate). Since the narrowest FWHM is approximately 470 ms (Fig. 3A, 4 Hz), electronic filtering is also likely contributing to peak broadening. Therefore, use of the data acquisition software presently provided with the commercial instrument does not seem adequate to detect individual particles.

3.3. Single component peaks

As discussed above, the spread of the FWHM distribution at 100 Hz (Fig. 3) suggests that not all the observed peaks are single component peaks (SCPs). We used the Statistical Overlap Theory (SOT) to estimate the number of SCPs, doublets, triplets, etc. that are found in an electropherogram. This theory, based on Poisson statistics, was originally developed to deal with complex chromatograms [20–27], but can be extended to the analysis of individual particles. In SOT, it is assumed that interval between the peaks (i.e. migration times) are purely probabilistic and can be used to predict the frequency of SCPs. It is indeed known that the intervals between peaks are deterministic quantities because they are defined by the separation conditions such as electric field, EOF, and buffer pH. However, the success of this theory in deterministic chromatographic separations suggests that it would be equally applicable to electrophoretic separations of individual particles.

In order to determine if the SOT can be applied to the data collected at 100 Hz, the distance between adjacent peaks (spacing) is sorted and then plotted versus peak number. If the spacing (S) fits an exponential curve, the SOT is an adequate model to describe SCPs. For instance, using S for the 16 observed peaks in Fig. 2A, trace 2, the exponential fit is $S(n) = (0.0006 \pm 0.0088) + (0.2047 \pm 0.0090) \times \exp[(-0.2014 \pm 0.0259) \times n]$, ($\chi^2 \sim 99.5\%$) where n is the number of peaks. Therefore, it is possible to use SOT for the data collected at 100 Hz. On the other hand, the data collected at 4 Hz data acquisition rate (e.g. Fig. 2A, trace 4 Hz) does not fit an exponential curve indicating that it is not possible to use the SOT for these data.

Since the SOT predicts that saturation (α) and the average minimum resolution required for separation (R^*) are independent if α is small (i.e. there are few multiple component peaks; $\alpha < 0.5$), it is important to estimate α first and determine if the simple overlap theory can be applied. In order to estimate α, it is necessary to estimate the minimum spacing for the separation between two adjacent peaks (x_0) and the peak capacity (n_c). For peaks of similar intensity, it is adequate to arbitrarily set $R^* = 0.5$ as was done by Davies et al. and in their SOT studies [25]. Given the median FWHM from distribution 100 Hz (Fig. 3) and assuming a Gaussian peak shape, the standard deviation (σ) of an SCP is $(0.425) \times (215\,\text{ms}) = 91\,\text{ms}$ (i.e. $\sigma = 0.425 \times \text{FWHM}$). The minimum spacing for separation of two adjacent SCP (x_0) is:

$$x_0 = 4\sigma R^* = 4(91)(0.5) = 182\,\text{ms} \tag{2}$$

By examining several electropherograms obtained at 100 Hz, the smallest observed value was $x_0 = 160$ ms (data not shown). The two adjacent peaks that defined this value were clearly distinguishable and suggested that $x_0 = 182$ ms is reasonable value to estimate α as is described below [25].

In order to determine n_c, the range X is defined as $X = (t_{mig})_{max} - (t_{mig})_{min}$ where each term represents the maximum and minimum migration times, respectively, and n_c is calculated as:

$$n_c = \frac{X}{x_0} \tag{3}$$

From Eq. (2) and the migration time range in Fig. 2A, trace 100 Hz, the peak capacity for 100 Hz is $n_c = 65/0.182 = 357$. Using this n_c value and the number of expected peaks (m_{ave}), α is calculated as:

$$\alpha = \frac{m_{ave}}{n_c} = \frac{32}{357} = 0.090 \tag{4}$$

Therefore, it can be assumed that α and R^* are independent of each other and the simple SOT can be used to estimate the degree of overlap in the electropherograms.

SOT postulates that the probability, P_1, that a component is an SCP is the product of two independent probabilities that the adjacent peaks lie beyond the distance x_0. This probability is calculated using the following formula:

$$P_1 = (e^{-\alpha})(e^{-\alpha}) = e^{-2\alpha} \tag{5}$$

Thus, $P_1 = e^{-2(0.090)} = 0.84$ and the number of expected SCPs is $32(0.84) = 26.9$. Similarly, the probability that any two adjacent components form a doublet (P_2) is the product of three independent probabilities that the two peaks lie within

Table 2
SOT parameters for 100 Hz sampling rate

Saturation factor (α)	0.090
Probability of singlets (P_1)	0.84
Probability of doublets (P_2)	0.07
Probability of triplets (P_3)	0.006
Number of singlets (s)	26.9
Number of doublets (d)	2.2
Number of triplets (t)	0.20
Number of observed peaks (P)	29.3
Number of detected peaks (m)	31.9

α is the saturation factor (cf. Eq. (4)), P_1 (cf. Eq. (5)), P_2 (cf. Eq. (6)), and P_3 (cf. Eq. (7)) are the probability of SCPs, doublets and triplets, respectively. s, d, and t are the number of SCPs, doublets and triplets, respectively. P is the predicted number of peaks and m is the predicted number of detected particles.

x_0, and is calculated as:

$$P_2 = (e^{-\alpha})(1 - e^{-\alpha})(e^{-\alpha}) = (e^{-2\alpha})(1 - e^{-\alpha}) \quad (6)$$

$P_2 = (0.84)(1-0.91) = 0.07$, and the number of predicted doublets would be $32(0.07) = 2.24$. Using a similar approach the probability of triplets is:

$$P_3 = (e^{-2\alpha})(1 - e^{-\alpha})^2 \quad (7)$$

$P_3 = (0.84)(1-0.91)^2 = 0.006$, and the number of predicted triplets would be $32(0.006) = 0.192$. Thus, the total number of predicted peaks (P) is $P = s + d + t + \ldots$ where s, d, and t are the number of SCPs, doublets and triplets, respectively. Using the data calculated above, $P = 26.9 + 2.2 + 0.2 \approx 29.3$ peaks and the total number of detected particles is $m = s + 2d + 3t = 1(26.9) + 2(2.2) + 3(0.2) \approx 31.9$. These data are summarized in Table 2. This prediction is in agreement with the calculated number of sampled particles.

3.4. Migration times

Migration times for each run at 100 (filled circles) and 4 Hz (open circles) are depicted in Fig. 4. The pooled individual migration times at 100 and 4 Hz were 214 ± 30 s (average $\pm$ S.D.) and 238 ± 45, respectively. These values are not statistically significant at 99% confidence level. For each separate CE run, the symbol represents the average migration time while the error bars represent the range of migration times for the detected particles. As discussed earlier, in addition to the variation in particle electrophoretic mobility within the sampled particles, sample plug length, residual interactions with the capillary walls, and ultimately diffusion may slightly contribute to the observed migration time ranges [3,19]. The average migration time range is larger for 4 Hz (90 s) than for 100 Hz (60 s). Although the same capillary was used for both sets of experiments, data collected at 4 Hz were collected last. EOF measurement before and after these sets of experiments showed a 4% increase. This change in EOF alone cannot explain the changes in the migration time range. However, EOF increase is usually attributed to degradation of the coating that then results in more adsorption of the latex particles to the capillary walls thus leads to longer migration times.

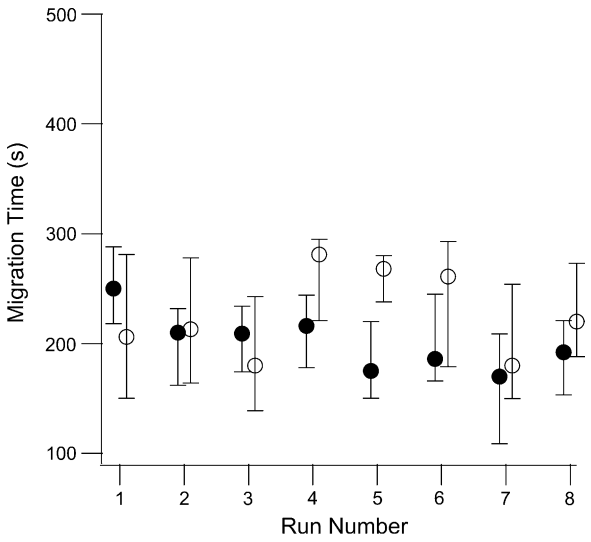

Fig. 4. Migration time reproducibility for 100 Hz (black circles), and 4 Hz (white circles). The upper part of the error bar represents the longest migration time for the run; and the lower part of the error bar represents the shortest migration time. All the experimental conditions are the same as Fig. 2. The data for 100 Hz is slightly offset along the x-axis for the sake of visual clarity.

Using the pooled data from eight consecutive runs obtained at 4 and 100 Hz, the average and the standard deviation for the calculated electrophoretic mobilities are $-(3.0 \pm 0.5) \times 10^{-4}$ and $-(3.3 \pm 0.8) \times 10^{-4}$ cm^2 V^{-1} s^{-1}, respectively. The corresponding electrophoretic mobility ranges are $-(3.7–2.5) \times 10^{-4}$ and $-(3.8–2.9) \times 10^{-4}$ cm^2 V^{-1} s^{-1}, respectively. These results indicate that the mobilities are less negative than previously reported values for latex particles of equal size (e.g. average electrophoretic mobility of -6.2×10^{-4} cm^2 V^{-1} s^{-1} for separations in 10 mM borate, 10 mM SDS, pH 9.3 buffer) [3]. The more negative mobility in the latter case is expected because the negatively charged SDS binds to the particles impinging additional negative charges upon them and because of the higher buffer pH.

3.5. Signal intensity

Table 1 compares run-to-run variations in individual peak signal intensity for 4 and 100 Hz. For all CE runs, the signal intensity R.S.D.s at 100 Hz are lower than those of 4 Hz. They varied from 20 to 33% for 100 Hz and from 35 to 70% for 4 Hz.

The signal intensity reproducibility for on-column LIF detection coupled with 100 Hz data acquisition rates is similar to those of sheath flow post-column LIF detectors, reported previously [3]. These post-column LIF detectors had signal intensity R.S.D.s ranging from 25 to 35%. The expected peak intensity R.S.D. predicted from the manufacturer specifications is 12%. Also, at 100 Hz, there are sufficient data points to

describe a single peak (i.e. 61 ± 13; average ± S.D.) making it unlikely that this factor contributes to the observed variation in peak intensities. Therefore, the unaccounted variation in peak intensities may result from the heterogeneities at the detector volume in the laser beam intensity profile, particle trajectories, or a combination of these factors. Experimental improvements leading to a better reproducibility in peak intensity include the use of capillaries with a narrower inner diameter and more thorough characterization of particle fluorescence intensities using an independent technique (e.g. flow cytometry).

At 4 Hz, the high R.S.D. in signal intensity of individual peaks (35–70%) is not adequate to describe the intensity of individual particles. Peaks migrating <250 ms apart are likely to be detected as a single peak increasing variations in the observed peak intensities.

3.6. Signal-to-noise ratio and smoothing

Smoothing has been used to improve S/N ratio. Although new smoothing approaches such as wavelet transform are being introduced to analyze CE data [28], in this report we used binomial filtering because it is widely accepted and accessible in statistical packages. In this approach a contribution from neighboring points is weighted according to the coefficients from a binomial expansion [28–30]. Adequate smoothing of an electropherogram would result in an enhanced signal-to-noise ratio (S/N) without compromising peak width broadening. Binomial smoothing of data collected at 100 Hz improved S/N (Fig. 5A, squares) from the initial value of 80. The best S/N (∼160) was obtained after smoothing with a filter size of 400. On the other hand, for data collected at 4 Hz, smoothing worsened S/N (Fig. 5A, asterisks) in relationship to the initial value of 100. These results are expected because the data have already been processed using the highly efficient Caesar algorithm [31,32]. This algorithm is based on (i) defining the peaks using the first derivative of the signal; (ii) constructing a linear and noise-free baseline from the start and end points of the peak; (iii) constructing a median-filtered baseline for the regions not containing any peaks; and (iv) adding the identified peaks to the filtered data. The virtually noise-free baseline resulting from applying the Caesar algorithm (e.g. noise < 0.2% of the background) makes it impossible to further improve S/N when using a binomial filter and explains the trend shown in Fig. 5A for 4 Hz.

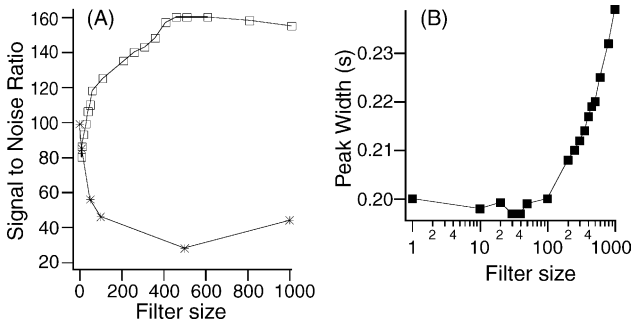

Fig. 5. The effect of binomial smoothing on signal-to-noise ratio and peak width. Panel A: average signal-to-noise ratio for data obtained at 100 Hz (squares) and 4 Hz (asterisks) smoothed with different filter sizes. Panel B: smoothing effect on peak widths for data acquired at 100 Hz. All experimental conditions are the same as Fig. 2.

Smoothing improves the S/N of the data acquired at 100 Hz, but S/N is still lower than custom-built CE systems with post-column LIF detection, which gives a S/N >300 for the same particle size (data not shown). This is expected because the post-column LIF detectors of the custom-built CE systems have lower scattering-associated noise than on-column LIF detectors. The former uses high optical quality flat quartz surfaces and a sheath flow instead of curved capillary walls to define the detection volume [33]. In addition, a decrease in the laser intensity transmitted through the fiber optics of the on-column LIF detector in the commercial instrument lowers the sensitivity of this detector.

As shown in Fig. 5B, the peak width for data collected at 100 Hz broadened with binomial smoothing [34]. Broadening is particularly detrimental for filter sizes >100. Therefore, smaller filter sizes are a good compromise to detect 1 μm diameter latex particles with an acceptable S/N. Using this filter size, the expected S/N and peak width are 140 and 210 ms, respectively. On the other hand, smoothing of data acquired at 4 Hz caused drastic broadening even when using a filter size of 10 (data not shown).

4. Conclusions

Using an external I/O board for data acquisition, it was possible to collect data at much higher sampling rates and take advantage of the automation of the commercial CE instrument for individual microsphere analysis. The use of an external data acquisition board also led to a better estimation of the true peak widths and the traveling time through the laser beam in the on-column LIF detector. Data acquired with external I/O board required additional smoothing to improve S/N. Binomial smoothing with a filter size of 100 is a good compromise for improving S/N ratio without causing excessive peak broadening. However, other smoothing procedures such as the Ceasar algorithm could be equally applied.

Without the use of an external data acquisition board, particles were detected as broad peaks. This broadening is believed to be the result of data bunching, the instrument response time, and further digital smoothing. It is believed that instrument manufacturers can easily address these issues and launch new software with features that will improve the compatibility of their present instrumentation with individual particle analysis. Use of the instrument modification reported here is an important step towards automated electrophoretic analyses of individual particles such as synthetic particles, organelles, viruses, bacteria, and other subcellular size systems.

Acknowledgement

Rahul Gupta (Department of Electrical Engineering, University of Minnesota) improved the algorithms for data analysis. Pete Carr provided insightful comments on SOT. E.A. acknowledges support from NIH (1K02-AG21453). This work was supported with NIH R01-GM61969.

References

[1] S.P. Radko, A. Chrambach, J. Chromatogr. B 722 (1999) 1.
[2] U. Schnabel, C.H. Fisher, E. Kenndler, J. Microcol. Sep. 9 (1997) 529.
[3] C.F. Duffy, A.A. McEathron, E.A. Arriaga, Electrophoresis 23 (2002) 2040.
[4] C.F. Duffy, S. Gafoor, D.P. Richards, H. Ahmadzadeh, R. O'Kennedy, E.A. Arriaga, Anal. Chem. 73 (2001) 1855.
[5] C.F. Duffy, K.M. Fuller, M.W. Malvey, R. O'Kennedy, E.A. Arriaga, Anal. Chem. 74 (2002) 171.
[6] E. Kenndler, D. Blass, Trends Anal. Chem. 20 (10) (2001) 543.
[7] D.W. Armstrong, L. He, Anal. Chem. 73 (2001) 4551.
[8] J. Zhang, K.O. Voss, D.F. Shaw, K.P. Roos, D.F. Lewis, J. Yan, R. Jiang, H. Ren, J.Y. Hou, Y. Fang, X. Puyang, H. Ahmadzadeh, N.J. Dovichi, Nucleic Acids Res. 27 (1999) e36.
[9] Y. He, W. Zhong, E.S. Yeung, J. Chromatogr. B 782 (2002) 331.
[10] M.A. Roberts, L. Locascio-Brown, W.A. MacCrehan, R. Durst, Anal. Chem. 68 (1996) 3434.
[11] S.P. Radko, M. Stastna, A. Chrambach, Electrophoresis 21 (2000) 3583.
[12] R.J. Hunter, Foundations in Colloid Science, Oxford University Press, 2001.
[13] Y.F. Cheng, N.J. Dovichi, Science 242 (1988) 562.
[14] C. Perrin, H. Fabre, D.L. Massart, Y. Vander Heyden, Electrophoresis 24 (2003) 2469.
[15] H. Ahmadzadeh, in: Instrumenation, Capillary Coating and Labeling Chemistry for Capillary Electrophoresis with Laser Induced Fluorescence Detection, University of Alberta, Alberta, 2000, p. 1.
[16] C. Gelfi, M. Curcio, P.G. Righetti, R. Sebastiano, A. Citterio, H. Ahmadzadeh, N.J. Dovichi, Electrophoresis 19 (1998) 1677.
[17] X. Huang, M.J. Gordon, R.N. Zare, Anal. Chem. 60 (1988) 1837.
[18] D.A. Skoog, D.M. West, H.F. James, Fundamentals of Analytical Chemistry, Saunders College Publishing, Fort Worth, 1996.
[19] S.P. Radko, A. Chrambach, J. Chromatogr. A 848 (1999) 443.
[20] J.M. Davis, J.C. Giddings, Anal. Chem. 55 (1983) 418.
[21] J.M. Davis, J.C. Giddings, J. Chromatogr. 289 (1984) 277.
[22] J.M. Davis, J.C. Giddings, Anal. Chem. 57 (1985) 2178.
[23] J.M. Davis, J.C. Giddings, Anal. Chem. 57 (1985) 2168.
[24] T.H. Seals, J.M. Davis, M.R. Murphy, K.W. Smith, W.C. Stevens, Anal. Chem. 70 (1998) 4549.
[25] J.M. Davis, M. Pompe, C. Samuel, Anal. Chem. 72 (2000) 5700.
[26] K.W. Smith, J.M. Davis, Anal. Chem. 74 (2002) 5969.
[27] C. Samuel, J.M. Davis, Anal. Chem. 74 (2002) 2293.
[28] B. Liu, Y. Sera, N. Matsubara, K. Otsuka, S. Terabe, Electrophoresis (2003) 3260.
[29] L. Cinotti, M. Meignan, J.P. Usdin, N. Vasile, A. Castaigne, J. Nucl. Med. 24 (1983) 768.
[30] M.A. King, P.W. Doherty, R.B. Schwinger, D.A. Jacobs, R.E. Kidder, T.R. Miller, J. Nucl. Med. 24 (1983) 1039.
[31] B. Coulter, Beckman P/ACE Setter Newsletter 4 (2000) 10.
[32] D. McKenzie, E. Bua, S. McKiernan, Z. Cao, J.M. Aiken, Eur. J. Biochem. 269 (2002) 2010.
[33] S. Wu, N.J. Dovichi, J. Chromatogr. 480 (1989) 141.
[34] W.H. Press, S.A. Teukolsky, W.T. Vetterling, B.P. Flannery, Numerical Recipes in C: The Art of Scientific Computing, Cambridge University Press, New York, 1977.